Journal of Alloys and Compounds 688 (2016) 594–598

Contents lists available at ScienceDirect

Journal of Alloys and Compounds

journal homepage: http://www.elsevier.com/locate/jalcom

Composition dependence of the Néel temperature and the entropy of the magnetic transition in the fcc phase of Fe-Mn and Fe-Mn-Co alloys

P. La Roca [a, b], P. Marinelli [a, c], A. Baruj [a, b, *], M. Sade [a, b], A. Fernández Guillermet [a, b]

[a] Centro Atómico Bariloche – CNEA, Instituto Balseiro (UN Cuyo), 8400, S.C.de Bariloche, Río Negro, Argentina
[b] Consejo Nacional de Investigaciones Científicas y Técnicas (CONICET), Argentina
[c] Ternium, Planta Gral. Savio, Casilla de Correo 801, 2900, San Nicolás, Argentina

ARTICLE INFO

Article history:
Received 14 June 2016
Received in revised form
18 July 2016
Accepted 19 July 2016
Available online 21 July 2016

Keywords:
Martensitic transformation
Antiferromagnetism
Thermodynamics
Modulated differential scanning calorimetry

ABSTRACT

A key feature of the fcc-to-hcp martensitic transformation (MT) in Fe-Mn based alloys is that the fcc structure is strongly stabilized by a paramagnetic-to-antiferromagnetic ordering reaction, which partially or completely inhibits the MT. In order to treat this phenomenon in thermodynamic terms it is necessary to account for the composition dependence of the Néel temperature (T_N) of the alloy and the entropy change (ΔS^{mg}) associated to the loss of the antiferromagnetic ordering. In the present work the composition dependence of these properties in Fe-Mn and Fe-Mn-Co alloys have been established by performing systematic measurements of the heat capacity. The current results are critically compared with experimental data from the literature, as well as estimates and correlations based on previous analyses by the present authors. The relevance of the reported data for the understanding of the fcc-to-hcp MT in the Fe-Mn and Fe-Mn-Co alloys is highlighted.

1. Introduction

Fe-Mn and Fe-Mn-X alloys (X = Si, Co, Cr) are characterized by the presence of two martensitic transformations (MTs) occurring on cooling, viz., the fcc-to-bcc (γ-α') and the fcc-to-hcp (γ-ε) MTs. Both of them are known to occur at temperatures which depend on the chemical composition of the alloys as well as on their microstructure. In particular, the fcc-to-hcp MT has attracted considerable attention for its interesting properties. For example, Fe-Mn-Si-X alloys with shape memory effect can recover deformations close to 8% [1], thus enabling the development of various types of technological applications [2]. Moreover, the deformation-induced fcc-to-hcp (γ-ε) MT in "high-manganese" Fe-Mn steels is an interesting phenomenon because this plasticity mechanism results in some beneficial functional and structural characteristics, such as high strength, ductility, strain hardening and elasto-plastic damping properties [3–6]. In particular, high-Mn alloys have been adopted to develop seismic control dampers in building constructions [7–9]. Moreover, Fe-Mn-Co alloys have long been suggested as an alternative for this application [10]. The low cost of these materials also contributes to increase the possibilities of their practical use.

In general, the thermodynamic analysis of the MT has often been performed by considering the Gibbs energy functions of the phases involved and the effect upon them of changes in key thermodynamic variables such as chemical composition, temperature, pressure and applied stress [11]. However, in order to establish reliable Gibbs energy functions (G_m), it is usually necessary to combine the thermodynamic properties of each individual phase with information on their relative stability provided by the phase diagrams [12–14].

The undercooled fcc structure in Fe-Mn and Fe-Mn-Co alloys is metastable in the temperature range where the MT occurs, and the hcp structure not a stable phase of the Fe-Mn phase diagram. As a consequence, a thermodynamic analysis of the MT in these systems cannot be based only upon information obtained under equilibrium conditions. Attempts have been made to obtain the necessary information by using the concept of T_o-temperature, i.e., the temperature at which the fcc and hcp phases with the same composition have the same G_m per mol. Even though T_o cannot be determined experimentally, it has often been treated as a quantity directly related to the temperature for the start of the fcc-to-hcp (M_s) and the hcp-to-fcc (A_s) transformations, e.g., as the average of M_s and A_s [15,16].

* Corresponding author. Centro Atómico Bariloche – CNEA, Instituto Balseiro (UN Cuyo), 8400, S.C.de Bariloche, Río Negro, Argentina.
E-mail address: baruj@cab.cnea.gov.ar (A. Baruj).

http://dx.doi.org/10.1016/j.jallcom.2016.07.213
0925-8388/

The calculation of T_o from the measured M_s and A_s temperatures becomes particularly challenging in Fe-Mn and Fe-Mn-X alloys due to the existence of a paramagnetic-to-antiferromagnetic ordering reaction which also occurs on cooling [17,18]. Specifically, it is accepted that the magnetic ordering reaction increases the stability of the fcc phase, and that it introduces significant negative deviations from linearity in the M_s versus composition functions at high Mn contents [15]. As a consequence, the T_o versus composition line cannot be determined by invoking the simplest $(M_s + A_s)/2$ rule. Instead, a full thermodynamic analysis of the M_s and A_s values accounting for the magnetic effect upon G_m of each of these phases, as well as the energy barriers to start the MTs is required [19,20].

Some years ago, such general methodology was applied to the Fe-Mn [16], the Fe-Mn-Si [19] and the Fe-Mn-Co [21,22] systems, by describing the magnetic contribution to G_m in terms of the classical model early suggested by Inden [23] and modified by Hillert and Jarl [24]. Those analyses indicated, in the first place, that the entropy change (ΔS^{mg}) associated to the antiferromagnetic-to-paramagnetic transition was strongly related to the observed decrease in the M_s temperatures. In particular, such relation allowed a refinement of the available [25] ΔS^{mg} versus composition function for the Fe-Mn system [15]. In the second place, a similar analysis of the Fe-Mn-Co system yielded a reasonably good account of the available data, but highlighted the need for T_N and ΔS^{mg} versus composition data to corroborate the interpolation and extrapolation schemes applied in the analysis [22].

The purpose of the present work is to obtain new experimental information on T_N and ΔS^{mg} for Fe-Mn and Fe-Mn-Co alloys. To this aim, measurements of the heat-capacity (C_p^{fcc}) of the fcc phase have been performed in the temperature range including the paramagnetic-to-antiferromagnetic transition. With this new information, ΔS^{mg} has been evaluated as a function of composition and compared with the results of previous studies [15,16,26] in the Fe-Mn system. Moreover, what seem to be the first experimental determinations of ΔS^{mg} for Fe-Mn-Co alloys, are reported in this paper.

In addition, the Néel temperature for several Fe-Mn and Fe-Mn-Co alloys has been established. With the present values, the composition dependence of T_N^{fcc} in the Fe-Mn and the Fe-Mn-Co system is discussed. In particular, the current values for Fe-Mn alloys are compared with the empirical T_N^{fcc} versus composition line suggested by Huang [25]. Moreover, the T_N^{fcc} results for Fe-Mn-Co alloys are combined with a previously adopted interpolation and extrapolation method [27] to develop an enlightening description of the systematic effect of the Co additions upon T_N^{fcc} of the Fe-Mn system.

2. Experimental procedure

Fe-Mn and Fe-Mn-Co alloys were prepared by melting the pure elements in an arc furnace under Ar atmosphere. Each individual alloy had the form of a button weighting approximately 13 g. The alloys were individually encapsulated in Vycor under Ar atmosphere, heat treated 48 h at 1273 K and subsequently quenched in water by breaking the capsules. Chemical composition measurements of all samples were performed by means of wave dispersive spectroscopy (WDS) using a Cameca SX-50 microprobe and including Fe, Mn and Co pure elements as standards. Small, flat calorimetric samples were obtained from each alloy and measured in Al crucibles provided by TA Instruments. Heat-capacity (C_P) measurements were performed in a TA Instruments 2910 modulated differential scanning calorimeter (MDSC) at constant pressure, under continuous Ar flow (18 sccm) [28]. Cooling and heating rates equal to 3 K/min were used in the temperature range from 100 K to 700 K, with a modulation characterized by a period of 100 s and amplitude of 0.5 K. The calibration of the MDSC cell was performed by using several pure elements and different heating rates. Specifically, the temperature, enthalpy changes, the base line and cell constant were calibrated by using the melting transition of Indium and Zinc as references. Besides, in order to obtain reliable C_P values, the so-called "C_P cell calibration constant" for the modulated type of measurement was obtained by using a sapphire sample. After performing these calibration procedures and in order to check the device performance, the C_P of a pure Fe sample was measured. The measurements agreed within less than 2% with the accepted values for Fe [29].

3. Measurements and assessed thermodynamic quantities

3.1. Fe-Mn alloys

The present heat-capacity (C_p^{fcc}) vs. T values corresponding to the Fe - 48.9 at.% Mn alloy are represented in Fig. 1 by a solid line. In this alloy the MT does not occur. The λ-shaped peak in C_p^{fcc} typical of the paramagnetic-to-antiferromagnetic transformation can be clearly observed. The Néel temperature T_N^{fcc} was defined as the inflexion point in the C_p^{fcc} vs. T curve measured on cooling. At temperatures higher than the indicated by the vertical dashed line, the fcc structure is paramagnetic.

In order to analyze the results in Fig. 1, it is useful to perform a phenomenological separation between the magnetic ($C_p^{mg,fcc}$) and non-magnetic ($C_p^{nmg,fcc}$) contributions to C_p^{fcc}, as suggested, e.g., by Hashimoto and Ishikawa [30]. The procedure involves the determination of a base line accounting approximately for the temperature dependence of the sum of vibrational and electronic contributions to the heat capacity. The non-magnetic contribution obtained by a smooth interpolation between experimental data well above and below T_N^{fcc}, is represented in Fig. 1 using a dashed line. Once the non-magnetic part is determined, the magnetic contribution to C_p^{fcc} was evaluated as follows:

$$C_p^{mg,fcc} = C_p^{fcc} - C_p^{nmg,fcc} \quad (1)$$

Using the $C_p^{mg,fcc}$ results, the entropy change associated to the antiferromagnetic order-disorder transition in the fcc phase, usually referred to as the "magnetic entropy" was determined as

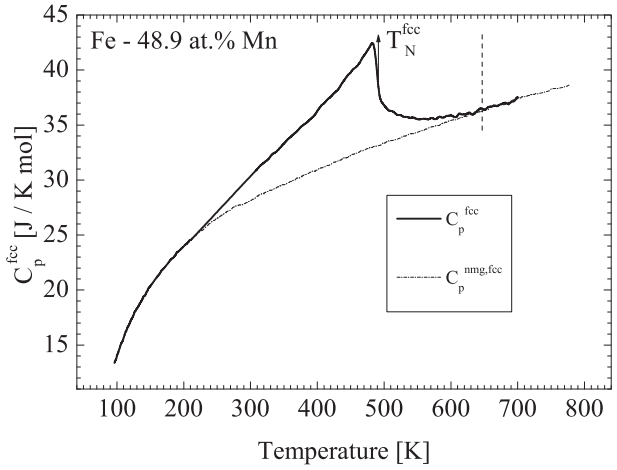

Fig. 1. Experimental C_p^{fcc} vs. T for a Fe - 48.9 at.% Mn (solid line). The dashed line represents the non-magnetic contribution $C_p^{nmg,fcc}$. The Néel temperature of the fcc phase (T_N^{fcc}) is indicated. At temperatures higher than the indicated by the vertical dashed line the fcc is paramagnetic.

suggested in Refs. [23,24], viz.,

$$\Delta S_m^{mg,fcc} = S_m^{mg,fcc}(\infty) - S_m^{mg,fcc}(0) = \int_0^{\infty} \frac{C_p^{mg,\,fcc}}{T} dT \qquad (2)$$

where T is the absolute temperature. For the present alloy, Eq. (2) yields. $\Delta S_m^{mg,\,fcc}\,(48.9Mn) = 2.51$ J/K.mol.

The experimental C_p^{fcc} vs. T for a Fe - 39.7 at.% Mn alloy is represented in Fig. 2 using a solid line. T_N^{fcc} is indicated in the figure, and the dotted line shows the non-magnetic heat-capacity. As in the case of Fig. 1, no structural transformation takes place in this alloy. The dashed line in Fig. 2 represents the experimental results by Hashimoto and Ishikawa [30], which have been included for comparison. The current C_p^{fcc} vs. T curve and that from Hashimoto and Ishikawa agree, in general, reasonably well, although the λ-shaped peak determined in their work is placed at a slightly lower temperature. In addition, the present measurements yield a better defined peak. In spite of these differences, the magnetic entropy value determined in the current study, viz., 2.72 J/K mol agrees with that reported by Hashimoto and Ishikawa within less than 9% [30].

The experimental and assessed thermodynamic quantities for the Fe-Mn alloys studied in the present work are listed in Table 1.

3.2. Fe-Mn-Co alloys

In order to study the effect of Co additions, the heat-capacity of three alloys with similar Mn content, viz., Fe – 28.4 at.% Mn, Fe – 28.2 at.% Mn – 3.5 at.% Co and Fe – 27.3 at.% Mn – 9.0 at.% Co, were studied. The results are listed in Table 1. The corresponding $C_p^{mg,\,fcc}$ values obtained by applying the procedure described above are plotted in Fig. 3 versus the T/T_N ratio. Considering that the alloys contain a similar amount of Mn (around 28 at.%), their main difference is in the Co contents. These results indicate that the maximum $C_p^{mg,\,fcc}$ value decreases when the Co content increases. The corresponding $\Delta S_m^{mg,fcc}$ (Table 1) also decreases.

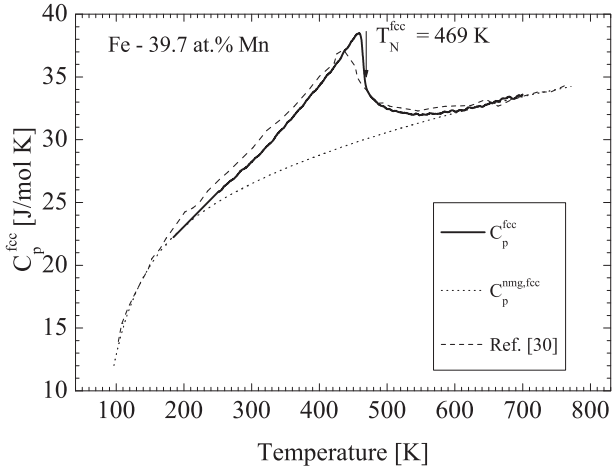

Fig. 2. Experimental C_p^{fcc} vs. T for a Fe – 39.7 at.% Mn (solid line). The dashed line represents the measurements reported by Hashimoto and Ishikawa [30] in a similar material. The dotted line corresponds to the non-magnetic contribution $C_p^{nmg,fcc}$. The Néel temperature of the fcc phase (T_N^{fcc}) is also indicated.

Table 1
T_N^{fcc} and $\Delta S_m^{mg,\,fcc}$ determined by MDSC measurements of C_p^{fcc} at constant pressure for various Fe-Mn and Fe-Mn-Co alloys.

%at. Mn	%at. Co	T_N^{fcc} [K]	$\Delta S_m^{mg,fcc}$ [J/K mol]
28.4	0.0	415 ± 5	3.22 ± 0.29
35.9	0.0	459 ± 5	3.26 ± 0.29
39.7	0.0	469 ± 5	2.72 ± 0.29
48.9	0.0	492 ± 5	2.51 ± 0.29
28.2	3.5	402 ± 5	2.38 ± 0.29
27.3	9.0	359 ± 5	1.88 ± 0.29
24.7	15.6	290 ± 5	–

4. Discussion

4.1. Composition dependence of the Néel temperature

The Néel temperature determined in the present work by measuring the heat-capacity of Fe-Mn alloys (filled symbols) are compared in Fig. 4 with the T_N vs. at.% Mn empirical expression obtained by Huang [25] by fitting to various types of experimental data (solid line). An excellent agreement is found, which adds to the credibility of the current calorimetric method.

In view of the agreement found in the Fe-Mn system, it is interesting to discuss the results for the Fe-Mn-Co since to the best of our knowledge, the only previous sources of ternary experimental T_N^{fcc} values are the work by Khomenko et al. [31] and by

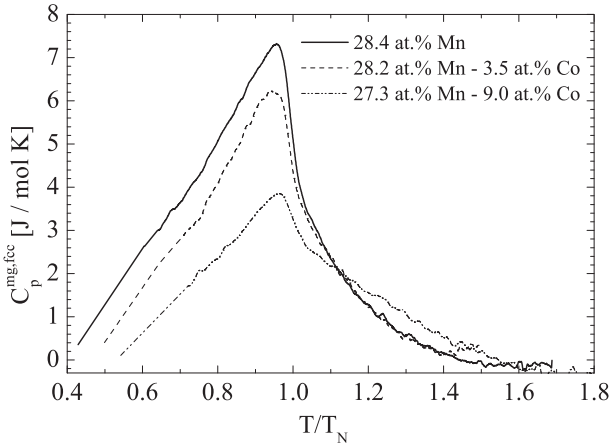

Fig. 3. $C_p^{mg,fcc}$ vs. T/T_N for alloys containing Fe-28.4 at.% Mn, Fe-28.2 at.% Mn-3.5 at.% Co and Fe-27.3 at.% Mn-9.0 at.% Co. The $C_p^{mg,fcc}$ curves were evaluated from the experimental results as explained in the text.

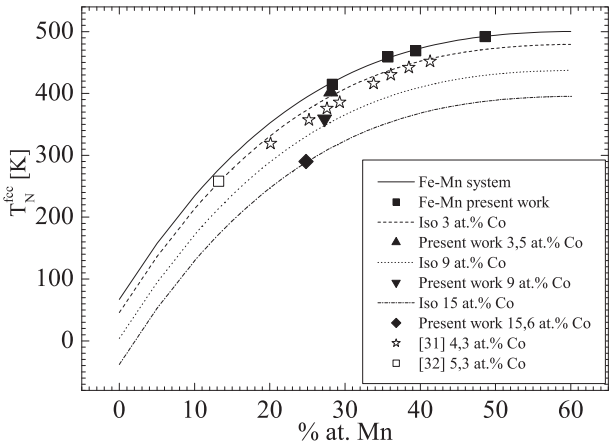

Fig. 4. The empirical T_N^{fcc} vs. at% Mn relation for Fe-Mn alloys due to Huang [25] (solid line) and those arrived at in the present work for Fe-Mn-Co alloys (3,9 and 15 at. %) using a procedure described in the text, compared with the present measurements and the results by Khomenko et al. [31] and by Yuksel and Agan [32] (empty symbols). The present measurements are plotted using filled symbols.

4.2. Fe-Mn-Co alloys

Yuksel and Agan [32]. A direct comparison with the values by Khomenko et al. cannot be made because the alloys studied by them differ in composition. Therefore, an indirect comparison procedure has been developed, which involves the use of the results by Khomenko et al. to construct probable T_N^{fcc} vs. Mn lines for selected Co contents. To this aim, linear extrapolations of their reported data were performed and used to evaluate the effect of Co additions upon the binary T_N vs. at.% Mn line proposed by Huang [25]. The T_N^{fcc} vs. Mn relations obtained in this way [27] for alloys with 3 at.% Co, 9 at.% Co and 15 at.% Co, are plotted in Fig. 4 using dashed and dotted lines. These lines are used in the following as a common reference for comparisons with the present and previously measured values (symbols).

The dashed and dotted lines in Fig. 4, which satisfactorily reproduce the results by Khomenko et al. [31], indicate that the addition of Co leads to a systematic shift to lower values of the TN vs. at.% Mn line, and that the magnitude of such an effect is well and consistently accounted for by the present measurements and the single measurement by Yuksel and Agan [32]. In view of the general agreement obtained it is suggested that the results in Fig. 4 provide a reliable basis for establishing the TN vs. composition relation needed to apply the Inden-Hillert-Jarl model to Fe-Mn-Co fcc alloys.

4.2. Composition dependence of the $\Delta S_m^{mg,fcc}$

A key result of the present work is the $\Delta S_m^{mg,fcc}$ associated to the antiferromagnetic-to-paramagnetic disorder transformation. The present $\Delta S_m^{mg,fcc}$ vs. at.% Mn results for Fe-Mn alloys are plotted using filled symbols in Fig. 5. A slight composition dependence is found, which might be represented using the following equation, obtained by a least-squares fit to the results in the (25–50) at.% Mn range:

$$\Delta S_m^{mg,fcc} = 1.043 - 0.009\, x_{Mn} \quad (3)$$

where x_{Mn} is the Mn content of the alloy expressed in at.%.

The current $\Delta S_m^{mg,fcc}$ vs. at.% Mn results are compared in Fig. 5

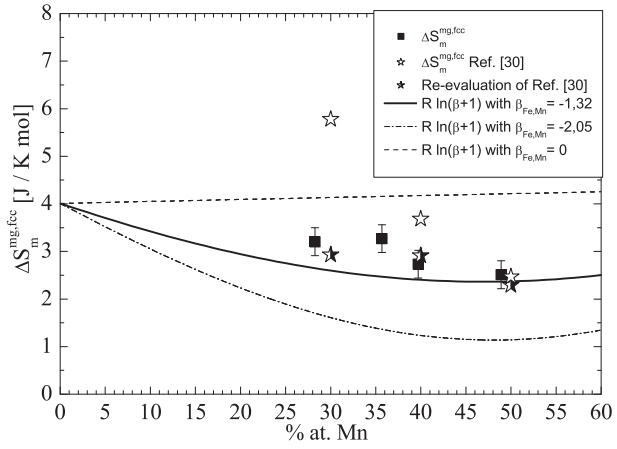

Fig. 5. Composition dependence of $\Delta S_m^{mg,fcc}$ in the Fe-Mn according to the present work (filled symbols) and other sources of information. Full star symbols represent the results reported by Hashimoto and Ishikawa [30]. Half-filled symbols represent the current re-evaluation of results from Hashimoto and Ishikawa. The additional lines represent the relations assessed by Huang [25] (dashed line), and by Cotes et al. using martensitic transformation data from Fe-Mn [15] (solid line) and Fe-Mn-Si [26] alloys (dashed-dotted lines).

with the values reported by Hashimoto and Ishikawa [30] from their own heat-capacity measurements (empty symbols) on alloys with 30, 40 and 50 at.% Mn. The comparison indicates that their result for the alloy with the largest Mn content is in excellent agreement with the present value for the alloy with 48.9 at.% Mn. However, their results for the alloys with 30 and 40 at.% Mn are significantly larger than the current ones, and indicate a strong decrease of $\Delta S_m^{mg,fcc}$ with increasing Mn content. In view of this striking discrepancy, additional pieces of information were included in the discussion, as explained in the following.

In the first place, considering that Hashimoto and Ishikawa presented their measured heat-capacity results in Ref. [30], their data were digitalized and re-evaluated by applying the same criteria used in the present work to determine the base-lines and non magnetic contributions to C_p^{fcc}. The corresponding $\Delta S_m^{mg,fcc}$ values are plotted in Fig. 5 using half-filled symbols, which evidently are very close to the results of present measurements.

In the second place, the composition dependence of the $\Delta S_m^{mg,fcc}$ values assessed by Cotes et al. [15] by analyzing MT temperatures was considered. They represented the magnetic entropy for elements and alloys using the expression $\Delta S_m^{mg,fcc} = R\ln(\beta+1)$ [23,24] where the dimensionless quantity β depends upon the Mn content. Lacking experimental information, β for Fe-Mn alloys had previously been described by Huang [25] as a linear interpolation between the values for the elements. The corresponding $\Delta S_m^{mg,fcc}$ values are represented in Fig. 5 using a dashed line which shows a slight positive slope. However, Cotes et al. showed that the analysis of MT temperatures and the T_o line allowed introducing a non-linear correction term of the form ($\beta_{Fe,Mn}\, x_{Fe}\, x_{Mn}$). By considering the MT results in the binary alloys they evaluated $\beta_{Fe,Mn} = -1.32$, which yields the $\Delta S_m^{mg,fcc}$ vs. at.% Mn function described by a solid line in Fig. 5. Evidently, the correction by Cotes et al. [15,16] to the linearly interpolated β led to entropy values in remarkably good agreement with the $\Delta S_m^{mg,fcc}$ values based on the current measurements and with those re-evaluated in the present study from the original heat-capacity data reported by Hashimoto and Ishikawa [30].

In closing this section, it should be mentioned that in a later work Cotes et al. re-evaluated the $\beta_{Fe,Mn}$ parameter by treating an extended database containing MT temperatures of Fe-Mn and Fe-Mn-Si alloys [26]. The result, $\beta_{Fe,Mn} = -2.05$ leads to the $\Delta S_m^{mg,fcc}$ vs. at.% Mn values described in Fig. 5 by a dashed-dotted line. This line indicates that the treatment of the MT in Fe-Mn-Si alloys requires $\Delta S_m^{mg,fcc}$ values that are even smaller than those obtained by the usual interpolation procedures for β, which in their case [26] involved the descriptions of the Fe-Mn, Fe-Si and Mn-Si systems. Considering the binary $\Delta S_m^{mg,fcc}$ values determined in the present work, it can be hypothesized that the decreased $\beta_{Fe,Mn}$ parameter arrived at in Ref. [26] probably reflects the consequences upon the optimized binary parameters of trying to accommodate a seemingly strong effect of Si upon $\Delta S_m^{mg,fcc}$ of the Fe-Mn-rich ternary alloys. New heat-capacity measurements in Fe-Mn-Si alloys would help to test this hypothesis.

The effect of Co additions upon $\Delta S_m^{mg,fcc}$ for Fe – 28 at.% Mn – Co alloys is presented in Fig. 6. The filled symbols represent the values obtained from the current measurements. The dotted line represents a linear fit to the results in Table 1. No previous determinations of $\Delta S_m^{mg,fcc}$ in this system have been found by us. The present results should therefore be considered as a valuable first contribution to the characterization of the magnetic transition in fcc Fe-Mn-Co alloys.

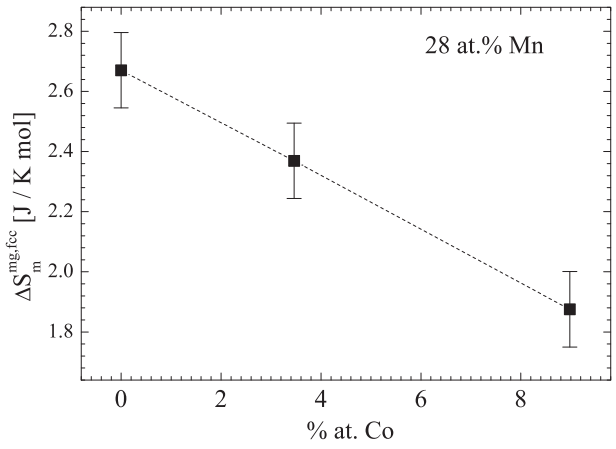

Fig. 6. The effect of Co additions upon $\Delta S_m^{mg,fcc}$ for Fe − 28 at.% Mn − Co alloys. The filled symbols represent the values obtained from the current measurements. The dotted line represents a linear fit to the results reported in Table 1.

5. Summary and concluding remarks

It has long been accepted that magnetism plays a key role in determining the phase stability of Fe-based alloys. More recent studies have shown that a quantitative account of the entropy change associated to the antiferromagnetic-to-paramagnetic transition is necessary in a detailed description of the martensitic transformation temperatures in Fe-Mn and Fe-Mn-X systems. In the present work new information has been presented concerning the fcc structure of Fe-Mn and Fe-Mn-Co alloys, viz., the composition dependence of the Néel temperature and the entropy of the antiferromagnetic-to-paramagnetic transition. The entropy results for fcc Fe-Mn alloys are found to agree remarkably well with the values extracted from MT temperatures in the binary system by using the Inden-Hillert-Jarl thermodynamic model. In addition, it is shown that the present Néel temperature results are consistent with the recommended values for Fe-Mn alloys and with the scarce previously published information on the Fe-Mn-Co system. In view of these facts, it is concluded that the current findings represent a valuable contribution to the understanding of the thermodynamics of the structural and magnetic transitions involving the fcc phase in Fe-Mn and Fe-Mn-Co alloys.

Acknowledgments

This work has been supported by Comisión Nacional de Energía Atómica, by Consejo Nacional de Investigaciones Científicas y Técnicas of Argentina (PIP 2011-00056), by Agencia Nacional de Promoción Científica y Tecnológica (PICT 2012-0884) and by Universidad Nacional de Cuyo (06-C452 and 06-C453).

References

[1] Y.H. Wen, H.B. Peng, D. Raabe, I. Gutierrez-Urrutia, J. Chen, Y.Y. Du, Large recovery strain in Fe-Mn-Si-based shape memory steels obtained by engineering annealing twin boundaries, Nat. Commun. 5 (2014) art. 4964.
[2] A. Sato, H. Kubo, T. Maruyama, Mechanical properties of Fe-Mn-Si based SMA and the application, Mater. Trans. 47 (2006) 571–579.
[3] O. Grässel, L. Krüger, G. Frommeyer, L.W. Meyer, High strength Fe-Mn-(Al, Si) TRIP/TWIP steels development - properties – application, Int. J. Plast. 16 (2000) 1391–1409.
[4] I. Nikulin, T. Sawaguchi, K. Tsuzaki, Effect of alloying composition on low-cycle fatigue properties and microstructure of Fe-30Mn-(6-x)Si-xAl TRIP/TWIP alloys, Mater. Sci. Eng. A 587 (2013) 192–200.
[5] J. Millán, S. Sandlobes, A. Al-Zubi, T. Hickel, P. Choi, J. Neugebauer, D. Ponge, D. Raabe, Designing Heusler nanoprecipitates by elastic misfit stabilization in Fe-Mn maraging steels, Acta Mater. 76 (2014) 94–105.
[6] A. Cladera, B. Weber, C. Leinenbach, C. Czaderski, M. Shahverdi, M. Motavalli, Iron-based shape memory alloys for civil engineering structures: an overview, Constr. Build. Mater. 63 (2014) 281–293.
[7] T. Sawaguchi, P. Sahu, T. Kikuchi, K. Ogawa, S. Kajiwara, A. Kushibe, M. Higashino, T. Ogawa, Vibration mitigation by the reversible fcc/hcp martensitic transformation during cyclic tension compression loading of an Fe-Mn-Si-based shape memory alloy, Scr. Mater. 54 (2006), 1885–1990.
[8] T. Sawaguchi, L.-G. Bujoreanu, T. Kikuchi, K. Ogawa, M. Koyama, M. Murakami, Mechanism of reversible transformation-induced plasticity of Fe-Mn-Si shape memory alloys, Scr. Mater. 59 (2008) 826–829.
[9] T. Sawaguchi, I. Nikulin, K. Ogawa, K. Sekido, S. Takamori, T. Maruyama, Y. Chiba, A. Kushibe, Y. Inouec, K. Tsuzaki, Designing Fe-Mn-Si alloys with improved low-cycle fatigue lives, Scr. Mater. 99 (2015) 49–52.
[10] J.H. Jun, D.K. Kong, C.S. Choi, The influence of Co on damping capacity of Fe-Mn-Co alloys, Mater. Res. Bull. 33 (1998) 1419–1425.
[11] K. Otsuka, C.M. Wayman, in: K. Otsuka, C.M. Wayman (Eds.), Chapter 1, in Shape Memory Materials, Cambridge University Press, 1998.
[12] L. Kaufman, M. Cohen, Thermodynamics and kinetics of martensitic transformations, Prog. Met. Phys. 7 (1958) 165–246.
[13] A. Fernández Guillermet, Critical evaluation of the thermodynamic properties of cobalt, Int. J. Thermophys. 8 (1987) 481–510.
[14] L. Kaufman, M. Hillert, in: G.B. Olson, W.S. Owen (Eds.), Martensite, ASM International, Materials Park, OH, 1992, pp. 41–58.
[15] S. Cotes, M. Sade, A. Fernández Guillermet, Fcc/Hcp martensitic transformation in the Fe-Mn system: experimental study and thermodynamic analysis of phase stability, Metall. Mater. Trans. A 26 (1995) 1957–1969.
[16] S. Cotes, A. Baruj, M. Sade, A. Fernández Guillermet, Thermodynamics of the γ/ε martensitic transformation in Fe-Mn alloys: modelling of the driving force, and calculation of the M_s and A_s temperatures, J. Phys. IV Colloq. C2 Suppl. J. Phys. III 5 (1995) 83–88.
[17] A. Rabinkin, M. Ron, F. Trichter, E. Gartstein, On the γ/ε phase transformation in Fe-Mn alloys induced by high pressure and plastic deformation, in: Proc. Int. Conf. on Martensitic Transformations, ICOMAT 79, Cambridge, MA, 1979, p. 300.
[18] A.P. Miodownik, The role of anti-ferromagnetism on γ-ε transformation in Fe-Mn alloys, Z. Met. 89 (1998) 840–846.
[19] S. Cotes, A. Fernández Guillermet, M. Sade, Gibbs energy modelling of the driving forces and calculation of the fcc/hcp martensitic transformation temperatures in Fe-Mn and Fe-Mn-Si alloys, Mat. Sci. Eng. A 273–275 (1999) 503–506.
[20] S. Cotes, A. Fernández Guillermet, M. Sade, Fcc/Hcp martensitic transformation in the Fe-Mn system: Part II. Driving force and thermodynamics of the nucleation process, Metall. Mater. Trans. A 35 (2004) 83–91.
[21] A. Baruj, S. Cotes, M. Sade, A. Fernández Guillermet, Coupling binary and ternary information in assessing the fcc/hcp relative phase stability and martensitic transformation in Fe-Mn-Co and Fe-Mn-Si alloys, J. Phys. IV Colloq. C8 Suppl. J. Phys. III 5 (1995) 373–378.
[22] A. Baruj, A. Fernández Guillermet, M. Sade, The fcc/hcp relative phase stability in the Fe-Mn-Co system: martensitic transformation temperatures, assessment of Gibbs energies and thermodynamic calculation of T_0 lines, J. Phys. IV Fr. 7 Colloq. C5 Suppl. J. Phys. III (1997) 405–410.
[23] G. Inden, The role of magnetism in the calculation of phase diagrams, Phys. B 103 (1981) 82–100.
[24] M. Hillert, M. Jarl, A model for alloying in ferromagnetic metals, CALPHAD 2 (1978) 227–238.
[25] W. Huang, An assessment of the Fe-Mn system, CALPHAD 13 (1989) 243–252.
[26] S. Cotes, A. Fernández Guillermet, M. Sade, Phase stability and fcc/hcp martensitic transformation in Fe-Mn-Si alloys: Part II. Thermodynamic modelling of the driving forces and the M_s and A_s temperatures, J. Alloys Comp. 280 (1998) 168–177.
[27] A. Baruj: Ph.D. Thesis, Instituto Balseiro, U.N. Cuyo (1999) (http://ricabib.cab.cnea.gov.ar/81/1/Baruj_Tesis_vf.pdf).
[28] P.S. Gill, S.R. Sauerbrunn, M. Reading, Modulated differential scanning calorimetry, J. Therm. Anal. 40 (1993) 931–939.
[29] P.D. Desai, Thermodynamic properties of iron and silicon, J. Phys. Chem. Ref. Data 15 (1986) 967–983.
[30] T. Hashimoto, Y. Ishikawa, Antiferromagnetism of γ-FeMn alloys. III. Specific heat and thermoelectric power studies, J. Phys. Soc. Jpn. 23 (1967) 213–223.
[31] O.A. Khomenko, I.F. Khiĺkevich, G.Ye Zvigintseva, Influence of a third component on the Néel point of iron-manganese invars, Fiz. Metal. Metalloved. 37 (1974) 1325–1326.
[32] M. Yuksel, S. Agan, Magnetic transitions and the magnetic characteristics of the martensitic transformations in a Fe-Mn-Co alloy, Gazi Univ. J. Sci. 25 (2012) 323–326.